Lab on a Chip

RSC Publishing

CRITICAL REVIEW

Fabrication and multifunction integration of microfluidic chips by femtosecond laser direct writing

Cite this: *Lab Chip*, 2013, **13**, 1677

Bin-Bin Xu,[a] Yong-Lai Zhang,*[a] Hong Xia,[a] Wen-Fei Dong,[a] Hong Ding[c] and Hong-Bo Sun*[ab]

Received 5th November 2012,
Accepted 25th February 2013

DOI: 10.1039/c3lc50160d

www.rsc.org/loc

In the pursuit of modern microfluidic chips with multifunction integration, micronanofabrication techniques play an increasingly important role. Despite the fact that conventional fabrication approaches such as lithography, imprinting and soft lithography have been widely used for the preparation of microfluidic chips, it is still challenging to achieve complex microfluidic chips with multifunction integration. Therefore, novel micronanofabrication approaches that could be used to achieve this end are highly desired. As a powerful 3D processing tool, femtosecond laser fabrication shows great potential to endow general microfluidic chips with multifunctional units. In this review, we briefly introduce the fundamental principles of femtosecond laser micronanofabrication. With the help of laser techniques, both the preparation and functionalization of advanced microfluidic chips are summarized. Finally, the current challenges and future perspective of this dynamic field are discussed based on our own opinion.

Introduction

Ever since the mid-1990s, micro total analysis systems (μTAS), or so-called 'lab-on-a-chip' (LoC) devices have been considered an up-and-coming technique; they have been recognized as one of the world-changing technologies; Nature magazine has deemed them to be the technology of this century.[1–7] To date, despite a short history (~20 years), microfluidic techniques, represented by LoC systems, have revealed a cornucopia of both new fluidic physics and various scientific applications in

Bin-Bin Xu

Bin-Bin Xu received her BS in Electronic Science and Technology (2007) from Jilin University. She then worked as a volunteer teacher for one year in Kuerle city, Xinjiang Uygur Autonomous Region. She received an Outstanding Volunteer of China award. Since 2008, she has been a graduate student in Jilin University under the guidance of Prof. H. B. Sun in the State Key Laboratory of Integrated Optoelectronics. Her research is focused on the fabrication of metallic micronanostructures and their applications in SERS detection, advanced optoelectronic devices, and lab-on-a-chip systems.

Yong-Lai Zhang

Yong-Lai Zhang received his BS (2004) and PhD (2009) from Jilin University. After receiving his PhD, he joined the faculty in the State Key Laboratory on Integrated Optoelectronics, College of Electronic Science and Engineering, Jilin University. In 2011, he worked as a research professor in Yonsei University, Korea. He was then awarded a "Hong Kong Scholar" postdoctoral fellowship and worked at the Center of Super Diamond and Advanced Films (COSDAF), City University of Hong Kong. He is currently an associate professor in Jilin University. His research interests include laser micronanofabrication of functional structures, graphene-based microdevices and lab-on-a-chip systems.

---

[a] *State Key Laboratory on Integrated Optoelectronics, College of Electronic Science and Engineering, Jilin University, 2699 Qianjin Street, Changchun, 130012, P. R. China. E-mail: yonglaizhang@jlu.edu.cn; Fax: +86-431-85168281; Tel: +86-431-85168281*

[b] *College of Physics, Jilin University, 119 Jiefang Road, Changchun, 130023, P. R. China. E-mail: hbsun@jlu.edu.cn*

[c] *State Key Laboratory of Inorganic Synthesis and Preparative Chemistry, College of Chemistry, Jilin University, 2699 Qianjin Street, Changchun, 130012, P. R. China*

fields ranging from chemistry, physics, biology, materials science, pharmaceuticals and tissue engineering to iatrology. During the past two decades, microfluidic chips have revived interest in scaling laws and dimensionless groups for the basic purpose of downscaling.[7] By definition, microfluidics is the science and technology of systems that can process or manipulate ultra-small amounts of fluids by using microchannels with dimensions ranging from tens to hundreds of microns. Through the manipulation of microfluids in an interconnected microchannel, LoC systems can offer fundamentally new capabilities in the control of molecule concentrations both spatially and temporally.[2] More importantly, owing to the ultra-low reagent consumption in various reactions, LoC devices have revealed a series of practical benefits and distinct advantages, such as high activity, high sensitivity, safety, portability and environmental friendliness. Thus they not only provide an experimental platform for a wide range of chemical/biochemical reactions, but also contribute to high efficiency and sustainability.

Currently, with the rapid development of microfluidics, LoC systems have found broad applications in various aspects of experiments including synthesis, analysis, detection, separation, sensing, catalysis, and therapy. Especially, in some advanced biological research, for instance, immunoassays, tumor biopsy screening, genotyping, DNA amplification, nucleic acid concentration purification, gene therapy and DNA fragment-size determination,[8–14] microfluidic techniques play a very important role. More and more laboratory components with multifunctionality ranging from temperature control to microfluidic manipulation have involved LoC

Hong Xia

Hong Xia received her BS and PhD degrees in chemistry from Jilin University in 2001 and 2006. She joined the faculty in the State Key Laboratory on Integrated Optoelectronics, College of Electronic Science and Engineering, Jilin University in 2006. In 2010, she worked as a CRYST fellow in the National Institute for Materials Science, Japan. She is currently an associate professor in Jilin University. Her research is focused on the synthesis of optical and magnetic functional materials, and micronanofabrication by lasers based on functional resins and polymers.

Wen-Fei Dong

Wen-Fei Dong received his PhD (2004) from the Department of Interfaces, Max-Planck-Institute of Colloids and Interfaces, Germany under the supervision of Prof. Helmuth Möhwald. From 2006 to 2008, he joined the group of Prof. Kataoka Kazunori in the University of Tokyo as a JSPS postdoctoral fellow. He received the "Asia Excellence young researcher" award from the President of the Polymer Society of Japan. He then moved to the State Key Laboratory on Integrated Optoelectronics, College of Electronic Science and Engineering, Jilin University as an associate professor. His recent research projects focus on self-assembly, multifunctional nanoparticles, novel biosensors and laser-based biofabrication.

Hong Ding

Hong Ding worked as a senior engineer in the State Key Laboratory of Inorganic Synthesis and Preparative Chemistry, Jilin University, from 1983 to 2004. Since then she has been a researcher of chemistry at Jilin University. Her work is primarily focused on in situ analysis of catalytic reactions through advanced techniques including in situ IR spectroscopy, on-chip fluorescence spectroscopy, and lab-on-a-chip systems.

Hong-Bo Sun

Hong-Bo Sun received his PhD from Jilin University in 1996. He worked as a postdoctoral researcher at the University of Tokushima, Japan, from 1996 to 2000, and then as an assistant professor in the Department of Applied Physics, Osaka University. He became a project leader in 2001. He was awarded by the Optical Science and Technology Society in 2002, and won an Outstanding Young Scientist Award issued by the minister of MEXT (Japan) in 2006. In 2005, he became a professor (Changjiang Scholar) at Jilin University. His research is focused on laser micronanofabrication, and its application in microoptics, micromachines, microfluids, and microsensors.

systems. As reported by Mathies *et al.*, a chip-based bioprocessor integrated multifunctional units such as 250 nL reactors, affinity-capture purification chambers, high-performance capillary electrophoresis channels, and pneumatic valves and pumps onto a single microchip to realize three Sanger sequencing steps including thermal cycling, sample purification, and capillary electrophoresis.[15] Qin *et al.* presented a novel microfluidic device integrated with 48 hybridization units containing 48 microvalves and 96 micropumps for the automation of shuttle flow to realize rapid DNA hybridization.[16] The gradually increasing applications of LoC devices have placed higher requirements on chip functionality and compatibility.[15,17]

Additionally, in the pursuit of smaller sizes and higher integration, there is a growing interest in the preparation and functionalization of modern microfluidic chips by using novel processing techniques. According to the reported results, most of the multifunctional microfluidic chips are manufactured through classical ''top-down'' and ''bottom-up'' approaches. For instance, injection molding, casting, hot embossing, thermal forming, ultraviolet (UV), e-beam, X-ray lithography, and nanoimprinting have been successfully adopted for the fabrication of functional microchips.[18–23] However, the abovementioned technologies are somewhat powerless when facing complex microstructures, especially 3-dimensional (3D) units. Moreover, these micronanofabrication techniques are incapable of integrating functional structures inside a given microfluidic chip due to nonplanar microchannel networks. From the technical point of view, the development of microfluidics shows a certain dependence on the state-of-the-art of micronanofabrication techniques. Consequently, there is an urgent need for a flexible and tunable processing technique which is suitable for chip preparation and functionalization.

In recent years, femtosecond laser micronanofabrication has shown special capability for prototyping 3D micronanostructures[24,25] by using a wide range of photosensitive materials.[26–34] The programmable designability, 3D processing capability, high spatial resolution and accuracy make femtosecond laser processing a promising enabler for both the fabrication and functionalization of microfluidic chips.[35,36] In this review, we highlight the contributions of this powerful technique to the field of microfluidics. Firstly, the fundamental principles of femtosecond laser fabrication including both subtraction-type and addition-type micromachining are introduced briefly. Then, the femtosecond laser fabrication technique used in the preparation of functional microfluidic chips is discussed. In addition, the paper also reviews recent developments in the post integration of various functional devices including microsieves, microvalves, overpass structures, micromixers, microheaters, SERS monitors and catalytic reactors inside microfluidic chips by using this technique.[26,29,33,37–42] Finally, both the current challenges and future perspective of this powerful technique in the field of microfluidics are discussed based on our own opinion.

Fundamental principles of femtosecond laser direct writing (FsLDW)

Subtraction-type FsLDW: latent image writing followed by etching

In femtosecond laser micromachining, pulses from a femtosecond laser are used to create microstructures on the surface or in the bulk of solid materials. Generally, the most common laser system used for micromachining is the Ti:sapphire laser. This type of laser uses a titanium-doped sapphire crystal as the gain medium, and has a center wavelength of near 800 nm. Recently, femtosecond laser systems of around 1 μm wavelength based on fibers, Yb:YAG, Yb:KGW, Yb:KYW, have become more widely used.[43,44] Typically, FsLDW induced latent imaging followed by an etching process, here called subtraction-type FsLDW, has been widely used for micromachining; this technique shows many unique advantages. First, the ultrafast pulse ranging from tens to hundreds of femtoseconds can effectively suppress the heat-affected zone in the laser scanning region, because the energy deposition generally occurs on a timescale that is much shorter than that of other relaxation processes. In this regard, femtosecond laser micromachining is generally considered as a cold processing tool.[45] Besides, the interaction between materials and the femtosecond laser pulses differs from that with other laser sources, such as continuous wave light. The intensity of a femtosecond pulse, even with very moderate energy, is high enough to drive a nonlinear absorption process in materials that do not normally absorb at the laser wavelength.[46,47] Typically, when a single photon does not have enough energy to excite an electron from the valence to the conduction band, absorption of laser energy can occur through a nonlinear process, which is known as multiphoton absorption.[48,49] This nonlinear absorption allows not only 3D microfabrication with a spatial resolution far beyond the optical diffraction limit to be achieved, but also processing capability towards a wide range of materials including both soft polymeric materials[50–54] and hard inorganic materials.[46,55–59] In typical subtraction-type FsLDW micromachining, chemical or physical properties of the target material are changed permanently in the laser irradiated region which is controlled by preprogrammed patterns. Taking advantage of the processing features, this technique could be used towards a wide range of materials through various photochemical/photophysical processes such as direct ablation and etching of an as-formed latent image. In the case of microfluidic chips, by pinpoint laser writing, photon energy is deposited along the laser-scanned traces, which then form latent images of LoC structures. The chemical activity of materials consisting of the LoC images is enhanced due to the energy deposition, which is easily removed by wet etching to form channels, chambers and other LoC geometries. In combination with the programmable processing capability, ultrafast laser micromachining can be used for the preparation of complex microfluidic chips in a designed manner, for instance 3D microfluidic chips.

Addition-type FsLDW: two-photon photopolymerization

Beside subtraction-type FsLDW, which is generally used to create desired microchannel structures from bulky chip materials, femtosecond lasers can also be used for chip preparation and integration through an addition-type FsLDW process, for example, two-photon photopolymerization (TPP). In a typical TPP process,[60,61] electron excitation of a photopolymer absorbs two near-infrared photons simultaneously in a single quantum event whose collective energy corresponds to the UV region of the spectrum, to realize transition from the ground state to an excited state, as shown in Fig. 1a. In this case, the rate of two-photon absorption (TPA) is proportional to the square of the light intensity, and thus TPA only occurs at the focal region where photon density is high enough. Consequently, TPP can be utilized to create 3D structures by scanning a tightly focused laser beam according to designed patterns from the bottom slice to the upside slice until the entire 3D structure is achieved, as shown in Fig. 1b. To date, TPA induced photopolymerization of photoresists has been a well established method for prototyping various micronanostructures.[62–66] The target microstructures are generally constructed based on photoresists whose ingredients include photoinitiators that are used for radical generation after excitation, monomers or oligomers that act as the main skeleton of micronanostructures, and cross-linkers that ensure insolubility in the developing solvents. Commercially available photoresists include two types, positive-tone and negative-tone photoresists, which can be applied to define the laser non-irradiated and irradiated regions, respectively. For practical usage, the composition of a photoresist might be more complex, for instance, multi-photoinitiators, photosensitizers and other functional molecules or doping agents could be included.[31,67,68] Moreover, the target structures are not limited to polymers, once an appropriate photochemical or photophysical scheme is developed, the process may be utilized for micronanofabrication. To date, besides photopolymers, microstructured metals, metal oxides, carbon material, proteins and composite materials have been readily fabricated through two- or multiphoton absorption processes.[36]

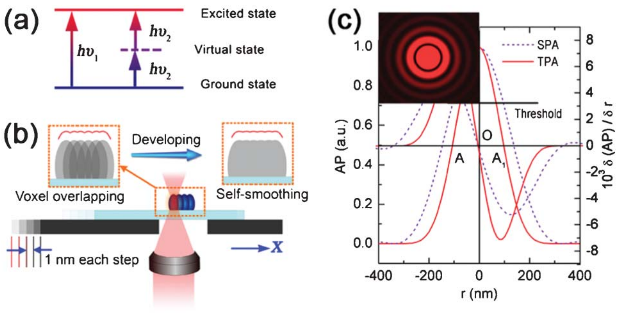

Fig. 1 (a) Schematic illustration of the TPA process. (b) Scheme of TPP fabrication. (c) Illustration of the achievement of sub-diffraction-limit (SDL) fabrication accuracy. The absorption probabilities for single photon absorption (SPA) and TPA are denoted by dashed and solid lines, respectively. The inset is a diffraction pattern. Reproduced from ref. 69 with the permission of AIP. ©2001 American Institute of Physics.

In addition to the broad processable materials, TPP fabrication also exhibits high spatial resolution, which can be attributed to the cooperation of several factors. Firstly, as mentioned previously, the laser beam is tightly focused by a high NA lens to form a very small focal spot where the photon density is high enough to induce photochemical reactions. Additionally, the ultrafast laser pulses, usually from tens to several hundreds of femtoseconds, can efficiently suppress heat diffusion, which also contributes to the high spatial resolution. In view of the rate of two-photon absorption being proportional to the square of the light intensity, which is spatially narrower than that of the linear one (Fig. 1c),[69] the nonlinear optical effect would result in a reduction of light–matter interactive volume, and lead to an improvement in fabrication resolution. Besides, the diffraction limit can be exceeded provided that the photochemical processes responsible for the formation of voxels have a threshold response to light excitation, as shown in Fig. 1c. The threshold is a level of light intensity, above which the photochemical reactions become irreversible. TPA-induced radicals can survive and initiate polymerization only at regions where the exposure energy is larger than the threshold. This effect is called chemical nonlinearity. For the particular case of the photopolymerization of resins, the unpolymerized monomer or photoinitiator molecules or molecular segments are removable from the polymer network. The removal of unsolidified materials is called materials nonlinearity. The synergetic effect of the above factors makes it possible to achieve reproducible fabrication resolution of tens of nanometres, at a level of $\lambda/10$ to $\lambda/50$, much smaller than the optical diffraction limit (ODL). Here, the ODL means that the resolving power is limited by Rayleigh's criterion, $\delta r = \kappa 1\lambda/\mathrm{NA}$ (κ is a constant depending on the laser linewidth and projection geometry; λ is the wavelength of the incident laser; NA is numerical aperture).[69]

In principle, the fabrication accuracy is generally determined by the smallest achievable voxel sizes, as discussed above, whereas higher precision has been achieved in practical model prototyping. In TPP fabrication, microstructures are built from voxels that can overlap with each other (Fig. 1b). So it is possible to achieve any desired microstructure larger than a voxel itself with high precision beyond the restriction of voxel size. Additionally, the high reproducibility of the shape and size of voxels and high positioning accuracy of voxels due to the usage of a piezo moving stage with motion accuracy better than 1 nm could also guarantee high precision.

Furthermore, TPP fabrication also exhibits other merits, for instance designability and 3D processing capability, as compared to conventional micronanofabrication approaches. All of these processing features make TPP fabrication a universal tool for both chip preparation and functionalization in a designed manner. Fig. 2 shows a schematic illustration of a TPP fabrication system used for chip functionalization. The system consists of five parts including a laser source, beam direction system, beam steering and motion stage, computer graphic generation and control system, as well as an *in situ* monitoring system. As a typical laser processing system, femtosecond-laser pulses were tightly focused on a desired position by a high-numerical-aperture (NA = 1.35, 100 ×) oil-immersion objective lens. The focal spot was scanned laterally

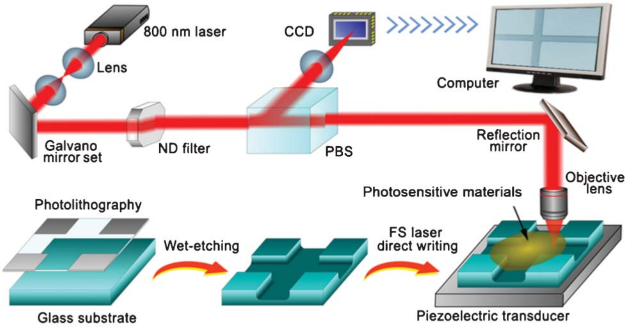

Fig. 2 Schematic illustration of a TPP fabrication system used for microfluidic chip preparation and functionalization. Reproduced from ref. 29 with the permission of RSC. ©2012 by the Royal Society of Chemistry.

by steering a two-galvanomirror set, and moved vertically along the optical axis by a piezo stage, both with motion accuracy better than 1 nm. Under the guide of preprogrammed patterns, photosensitive materials placed on the chip could be irradiated by the focused femtosecond laser, inducing the formation of microstructures due to the variation of material properties.

Fabrication of microfluidic chips by FsLDW

Subtraction-type FsLDW for microfluidic chips

Femtosecond laser micromachining has long been considered as a powerful processing tool for the microstructuring of various materials. Typically, the ultrashort laser pulses can be used for the fabrication of microstructures through a direct ablation process or by an irradiation induced photochemical or photophysical change in the material properties, followed by an etching process.[70–72] Its strong processing capability makes femtosecond laser micromachining a technical support for both the fabrication and functionalization of microfluidic devices. In this section, we will briefly introduce the fabrication of both inorganic and polymeric microfluidic chips through the femtosecond laser micromachining technique.

Inorganic microfluidic chips

Femtosecond laser micromachining can be applied to a wide range of materials for the fabrication of microfluidic chips. Generally, in femtosecond laser ablation, three kinds of structural changes, including isotropic refractive index change;[73,74] birefringent refractive index change;[75,76] and void formation,[77–79] have been successfully developed for laser micromachining in the bulk of transparent materials. For the fabrication of inorganic microfluidic chips, both the laser parameters (*e.g.*, pulse duration, wavelength, energy, repetition rate), and material parameters (*e.g.*, bandgap, thermal properties) show a certain influence on the structure morphology. In this case, high quality materials processing without visible thermal and mechanical damage can be achieved using ultrashort laser pulses at low fluences which are close to the ablation threshold.

To date, there exist many successful examples of the prototyping of hollow structures for microfluidic device preparation using femtosecond (fs) laser micromachining.[80–87] To the best of our knowledge, Misawa *et al.*, firstly reported the work of intravolume 3D microfabrication in high-purity silica glass by direct writing of a preprogrammed 3D pattern inside silica glass and subsequent etching of the optically damaged silica with HF acid.[71] When the deposited laser radiation power exceeds the optical damage threshold, microexplosion of the silica sample takes place. At the focal point, multiphoton absorption first generates free carrier plasma, which further absorbs light and results in secondary ionization of the silica. However, the as-prepared structure surface is usually very rough. Later, in order to improve the surface smoothness, additional processes such as oxyhydrogen (OH) flame polishing or post baking were performed.[85,86] Previous reports indicate that plasma pressure waves may be a causative factor of densification, and even of limited destruction of the silica. Postshock examination of the samples indicated that modifications in the structure arose from the changes in the average bridging angles of the SiO_4 tetrahedrons.[71] The configuration deformation of the oxygen's valance electrons could be considered in terms of the Lewis base, which is more chemically active in reactions with acids than in materials such as undensified silica. Additionally, in the laser microexplosion region, a penetrative silica structure would form, leading to greater exposure of the silica to the acid. As a result, the etching rate of the fs-laser modified region in the silica will be higher with respect to that of the undamaged silica, and thus designed structures could be created after HF acid etching.

In addition to the fabrication of desired microchannels, both microfluidic structures and microoptical structures can be easily integrated within a commercially available photosensitive glass.[88,89] Photosensitive glass is a crystal-clear glass that belongs to the lithium-silicate family of glasses and was first discovered by S. Donald Stookey in 1937. Nowadays, there exist over 5000 varieties of photosensitive glasses and one of the most famous commercial ones is manufactured by the SCHOTT Glass Corporation with a trade name of Foturan.[60] It comprises lithium aluminosilicate glass doped with trace amounts of silver and cerium. The cerium (Ce^{3+}) ions play an important role as a photosensitizer, which can release electrons after UV irradiation and the silver ions can be reduced to atoms. In subsequent heat treatment, silver nanoclusters form and act as nuclei around which the crystalline phase of lithium metasilicate grows in the glass matrix. As this crystalline phase of lithium metasilicate is much more soluble in a dilute solution of HF acid than the glass matrix, it can be preferentially etched away.[90,91] Kondo *et al.*, firstly demonstrated 3D microdrilling of photosensitive glass by a multiphoton absorption (MPA) process and produced straight and Y-branched holes in the glass sample, which was carried out much earlier than the work using fused silica.[92] Similar to micromachining based on pure fused silica or general glass, as shown in Fig. 3, femtosecond laser microfabrication based on photosensitive glass (Foturan) usually needs four steps: (i) femtosecond laser scanning or irradiation to form microchannels or device contours; (ii) thermal treatment of the whole Foturan glass around the

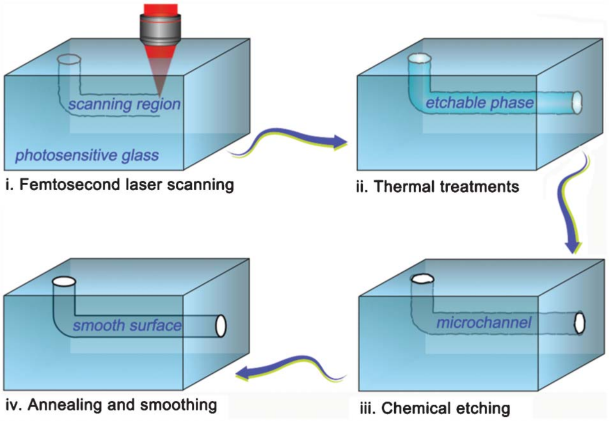

Fig. 3 Schematic illustration of the FsLDW fabrication of microfluidic chips based on photosensitive glass.

transition temperature; (iii) chemical wet etching; (iv) annealing for smoothing. In the first step, an oxidation reduction reaction occurs inside the glass during laser exposure, in which silver or gold ions are reduced to metal atoms. The second step is pivotal, in which thermal treatment leads to a transformation of the laser modified region into an etchable phase. Finally, after the etching and annealing process, desired microstructures could be readily fabricated inside the photosensitive glass chips.

Taking advantage of its 3D microfabrication capabilities, femtosecond laser micromachining can also be used to fabricate complex 3D microchannels.[93,94] For example, Li *et al.*, reported a spiral-shaped microchannel fabricated by FsLDW in glass. Hollow microstructures can be fabricated after hydrofluoric acid etching and post baking.[86,84] In addition, Cheng *et al.*, demonstrated the fabrication of a large-volume, square-shaped microfluidic chamber embedded in glass. After femtosecond laser micromachining in a porous glass substrate, the resultant sample was post-annealed at 1050–1150 °C, during which it could be sintered into a compact glass. Using this technique, a 1 mm × 1 mm × 100 μm microchamber and a square-wavelike channel with a total length of ∼1.4 cm and a diameter of ∼64 μm could be easily produced embedded beneath the glass surface separately.[93] The unique 3D structure of the microfluidic channel would enable good mixing of fluids as they pass through it. Therefore, it could act as a passive mixer.[90,94] Besides, Masuda *et al.*, reported a freely movable microplate integrated in the hollow structures embedded in photosensitive glass which could serve as a microvalve for the control of flow direction.[88]

Femtosecond micromachining is not limited to photosensitive glass; silicon can also be micromachined to form microchannels or chip-templates. For instance, silicon based multidepth microchannel networks have been successfully fabricated as a part of the development of artificial lungs by femtosecond laser ablation and subsequent acid etching.[72,92] In order to create efficient gas exchange and biocompatible flow conditions, Kam *et al.*, sought to replicate natural vascular networks fabricated as gas exchangers to mimic the natural vascular structure. The network was designed to bifurcate according to Murray's law and thus the channels become shallower and narrower at each bifurcation. Besides, Choi *et al.* reported that hot embossing mold patterns could be fabricated by femtosecond laser machining on AISI 304L stainless steel. To avoid the ablated materials redepositing onto the channel surface and obtain the best quality surface, a cross flow of argon gas was provided at 39×10^{-6} m^3 s^{-1} from a small nozzle.[95]

Moreover, the femtosecond micromachining technique allows the integration of high-quality optical devices and microfluidic channels on the same substrate such as glass, fused silica and photosensitive glass. The functional integration holds great promise for optical sensors, such as microlenses,[85] optical waveguides,[96,97] Fabry–Pérot interferometers,[84] Bragg grating waveguides[83,98] and so on. Tsai *et al.*, reported a simple Fabry–Pérot interferometer (FPI) embedded in a glass chip. The microdevice integrates a single-mode optical fiber and a microchannel in the photosensitive glass, and is capable of precisely measuring the refractive indices of liquid samples. The interference visibility is more than 4.0 dB, which is sufficient for most sensing applications.[84] Cerullo *et al.*, integrated optical waveguides into a commercial fused silica LoC device and demonstrated their capability to excite fluorescent molecules with high spatial selectivity in the manner of flowing inside microfluidic channels.[96]

In fact, the micromachining of inorganic materials is not limited to the use of femtosecond lasers. Nowadays, laser fabrication techniques that utilize high-energy ultraviolet (UV) excimer lasers with large-area homogenized beam cross sections also show distinct advantages including high resolution, high throughput, uniformity, highly localized heating, simplicity, and reproducibility. However, due to high absorptivity of native material at the excimer laser wavelength (UV region) and the large laser beam size, excimer lasers are more suitable for the fabrication of complex structures on surfaces. On the other hand, due to the low absorptivity at the laser wavelength (*e.g.*, ∼800 nm, ∼1 μm), femtosecond laser micromachining can be applied to a wide range of materials for the 3D machining or creation of microfluidic channels inside bulky solid materials. Despite the fact that femtosecond laser micromachining suffers from some drawbacks such as rough surface formation, disability in complex structures and low efficiency, it is still promising for chip fabrication and functionalization due to its strong processing capability and the diversity of suitable materials. Generally, a post surface polish would significantly improve the surface quality of the as prepared microstructures used in microfluidic devices.

Polymeric microfluidic chips

In addition to hard inorganic materials such as silicon, fused silica, glass and steel, polymeric materials including ethylene glycol dimethacrylate (EGDMA), poly(methylmethacrylate) (PMMA), poly(dimethylsiloxane) (PDMS), poly-*N*-methyl methacrylimide (PMMI), polycarbonate (PC), polyimide (PI) and polysiloxane are also suitable for laser processing.[50–54,99] As compared with inorganic microchips, polymers are more useful for some biomedical microfluidic devices, for instance, protein adsorption and cell cultivation.[54,99] In the treatment of polymeric materials, when the energy density of a focused femtosecond laser exceeds the level related to the molecular binding and ionization energies in the absorbing region, the polymer can be ablated from the surface, leading to the formation of 2D microfluidic channels. In this case, the use of a femtosecond laser is essential, because femtosecond laser micromachining can suppress thermal effects due to the ultrafast pulse which is shorter than the thermal diffusion time. In this regard, a comprehensive understanding of the interaction between a polymeric material and femtosecond pulses, paying particular attention to their pulse duration, energies, shapes, focusing conditions *etc.*, is indispensable. Based on the reported results, the widths of the resultant structures generally increase with input energy and scanning time, because the microstructures can be considered the result of the melting and re-solidification of the polymer at the high temperatures created by these intense, short pulses. With the help of femtosecond laser micromachining, 3D microfluidic chips based on polymers can also be achieved.[53] Among the processable polymers, PMMA- and PI-based microchips show the best quality, because the solubilities of PMMA and PI strongly increase after femtosecond laser modification. As compared with the micromachining of inorganic materials, the processing of polymers is not popular. Especially, with the development of soft lithography techniques, it is very convenient to prepare polymeric microfluidic devices, for instance PDMS chips, through the replication of a hard template.

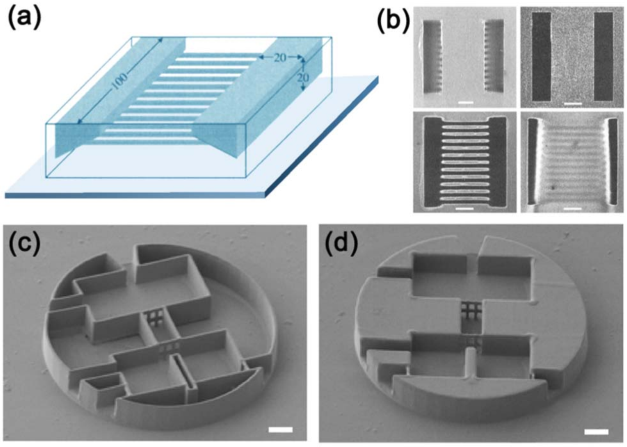

Fig. 4 Schematic illustration of a 3D microchannel structure fabricated by two-photon exposure of BSB-S2 in THPMA-MMA (positive-tone photoresists). (b) Scanning electron micrograph of the final structure, viewed normal to the substrate (upper, left) and two-photon fluorescence images of the final structure at and below the surface. The scale bar in (b) corresponds to 20 μm. Reproduced from ref. 102 with the permission of AAAS. (c) A conceptual microfluidic device fabricated by TPP of SU-8 (a negative-tone photoresist). SEM view image of the 3D microfluidic system (100 μm in diameter and 15 μm in height). Here, the internal portion of the background volume is solidified by additional ultraviolet exposure. (d) Two infiltration networks with six 2 mm sized bores. The scale bar is 10 μm. Reproduced from ref. 37 with the permission of RSC. ©2009 by the Royal Society of Chemistry.

TPP fabrication for microfluidic chips

For the fabrication of microfluidic chips, TPP also shows great potential.[46,100] In principle, the unique advantages of nanometre spatial resolution, 3D prototyping capability, and designability allow this technique to be used to fabricate any desired microstructure towards advanced microfluidic chips. However, from a practical point of view, the technique still suffers from the serious problems of high cost and long time consumption for the fabrication of an entire microfluidic device. In this regard, the use of positive-tone photoresists seems a good choice as the hollow-part occupies only a small proportion of a whole microfluidic chip. Zhou *et al.*, first demonstrated the fabrication of a microchannel structure by the TPP technique using BSB-S2 and THPMA-MMA as positive-tone photoresists. Fig. 4a shows the designed microfluidic structure which consists of two rectangular cavities (width, 100 μm; length, 20 μm; depth, 20 μm) and a sloped side wall that are connected by 12 microchannels (length, 50 μm; cross section, 4 μm by 4 μm lying 10 μm below the surface and spaced apart by 8 μm). As the microchannel structure was embedded in the polymer, it is difficult to distinguish the entire structures. However, two-photon fluorescence images focused at different depths from the film surface confirm the hollow channels and continuous connection to the cavities after removing the exposed region (Fig. 4b).[101]

In contrast, the use of negative resists suffers from much lower efficiencies, because a chip usually consists of various channels buried in a relatively large chip body. Point-by-point scanning processing using negative resists would lead to unreasonably low fabrication efficiencies. From the viewpoint of practical applications, despite the fact that commercial negative photoresists have better modeling and conformal capacities, the prolonged processing time in the direct laser writing constitutes one of the essential obstacles.[38] To solve this problem, Wu *et al.* proposed a profile scanning method for the prototyping of microfluidic chips using negative-tone photoresists. In their work, only the surface layer (shell) of a chip was polymerized through FsLDW, while the background was either removed by developer or solidified by additional ultraviolet exposure. The use of the solid photopolymer SU-8 was found to be critical for the formation of thin shells, as well as for the fabrication of suspended parts. The resultant structures are shown in Fig. 4c, d.[37]

Integration of multifunctional units with microfluidic chips

The wide application of microfluidic chips in chemical, biomedical and biological research or industrial fields calls for multifunctional chips with more complex systems and high integration. Thus, various micronanostructures based on a wide range of materials are highly desired at proper positions inside the microfluidic systems. Considering the non-planar property of the microfluidic chips, it is almost impossible to make complex structures inside the microchannels through conventional photolithography techniques. In this case, as a well established 3D nano-enabler, femtosecond laser fabrication shows great potential to solve this problem. The threedimensional processing capability, arbitrary-shape designability, wide array of processable materials and high fabrication accuracy up to tens of nanometres enable the femtosecond laser to integrate various 3D microstructures with commonly used microfluidic chips, making feasible the introduction of additional multifunctionality to general microfluidic channels. In this section, we briefly summarize the recent developments in the functionalization of microfluidic chips through femtosecond laser micronanofabrication.

Microsieves and one-way microvalves

In general microfluidic chips, the microchannel networks constitute the whole functionalities, including liquid sample injection, flow control, reagent delivery and mixing. However, for additional function extension, considerable difficulties arise for conventional micronanoprocessing techniques, despite only very simple structures being desired. For TPP fabrication, problems become easy to solve. In the first example, we represent microsieves and one-way microvalves.[26] By using TPP fabrication of photoresists (SU-8), Wang *et al.*, reported the embellishment of vertical microsieves inside a glass-based microfluidic channel. As shown in Fig. 5, microsieves with various pore shape and adjustable pore size were successfully fabricated inside a conventional glass-based microfluidic channel prepared by wet etching. It is worth pointing out that the fabrication of these simple structures with vertical arrangement relative to the substrate surface is almost impossible by conventional photolithography. The SEM images show that the microsieve wafers are ~1 μm in thickness and 15 μm in height. The pore shapes including round, square, round-end rectangle, pentagram, and equilateral triangle, could be easily created according to preprogrammed 3D structures. Although the shapes seem to be very simple, they include the basic building elements of various complex structures, including straight edges (edges of squares and triangles), cambered edges (round), acute angles (triangles), right angles (squares), obtuse angles, and angles with negative degree (pentagrams). In tests of sieve performance, particles smaller than the pore size can pass through a sieve; on the other hand, larger particles are headed off. With the help of this simple microsieve structure, additional functions such as particle screening, cell filtering and cell co-culture can be readily realized.

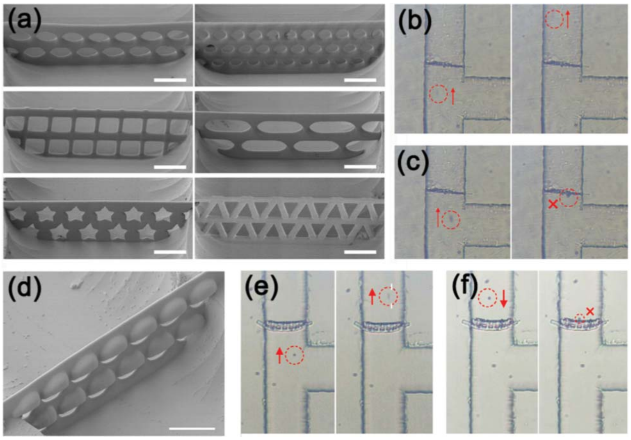

Fig. 5 (a) SEM images of microsieves with different pore sizes and shapes fabricated by TPP inside a glass-based microfluidic channel. (b) Optical microscopic images of the separation of microspheres using the microsieve. A sphere with a diameter smaller than the pore size could pass through the sieve, whereas a microsphere larger than the pore size could not pass through the sieve, as marked by the red circle in (c). (d) SEM image of a one-way microvalve. (e, f) Optical microscopic images of a test of the one-way microvalve. A microsphere could pass through the valve from the direction without eaves, but is headed off when flowing from the opposite direction, showing the one-way passing capability. The scale bars of the SEM images are 10 μm. Reproduced from ref. 26 with the permission of RSC. ©2010 by the Royal Society of Chemistry.

Similar to a microsieve, a microsieve with camber eaves was designed as a one-way valve for microfluidic chips (Fig. 5d). The unique filter wafer contained two major parts: a wall with 5.5 mm of round pores, and eaves half-covering the pores. When the particles come from the eave direction, they meet the eaves in advance, and lose their horizontal momentum. As a result, they bang against the eaves due to the flow force. On the other hand, if the particles come from the opposite direction, they lose horizontal momentum after passing the pores, and they then pass the valve with the microfluid flow. As confirmed by the recorded video, shown in Fig. 5e, f, this unique one-way microvalve was very employable, exhibiting favourable performance as expected.

Micro-overpass

In recent years, with the increasing complexity of microfluidic chips, there has been a growing interest in the development of 3D microchannels, which can realize more complex functionality such as solution mixing, light manipulation, 3D cell patterning, and even solving difficult problems computationally. Generally, a typical feature of a 3D microchip is that two microfluids can pass across the microchannel without mixing, and the basic principle for the fabrication of 3D microchannels is the precise assembly and ordered stacking of 2D patterned PDMS layers into a chip with 3D interconnectivity. For TPP fabrication, the realization of 3D flowing capability becomes much easier. Inspired from the overpasses that were constructed to regulate the traffic, He *et al.*,[29] reported the design and fabrication of a micro-overpass structure at the junction of crossed microchannels. With the help of the overpass structure, two microfluids in the conventional 2D microchannels could pass across the junction without mixing, illustrating the 3D flow capability. Fig. 6 shows the design principle of the overpass structure and the flow test of the 3D flowing performance. The overpass was designed into two layers which allow different microfluids to pass the junction, respectively. Fig. 6b shows the SU-8 overpass structure prepared by TPP fabrication. The performance of this overpass was evaluated by using two kinds of aqueous solutions with different colors (aqueous solutions of R6G and MB) as shown in Fig. 6c. With the help of post integrated overpass structures, the 2D microchannels show distinct 3D flow properties. The unique overpass structure at the junction of the 2D microchannels can be considered as an enabler to 3D microfluidic chips based on conventional 2D microchannels.

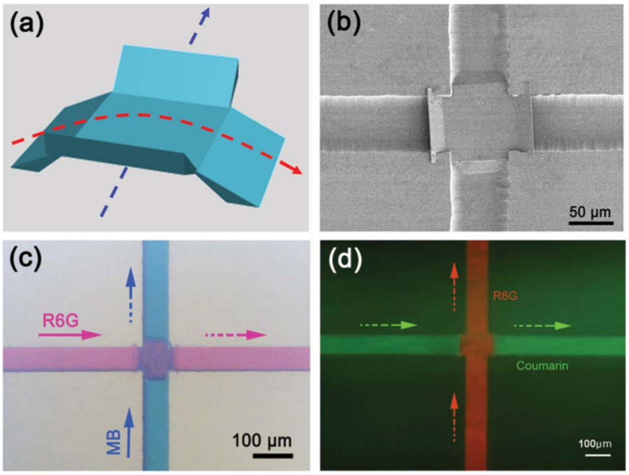

Fig. 6 Design and fabrication of an overpass microstructure at the junction of crossed microchannels. (a) 3D model of the designed overpass suitable for a two-channel crossed junction. (b) SEM image of the as-fabricated overpass microstructure at the junction of a glass-based crossed microchannel. (c) Flow test of two microfluids (R6G and MB). The two fluids can pass through the junction without mixing, indicating the 3D passing capability. (d) Fluorescent microscopic image of the R6G and coumarin solutions passing through the junction. Reproduced from ref. 29 with the permission of RSC. ©2012 by the Royal Society of Chemistry.

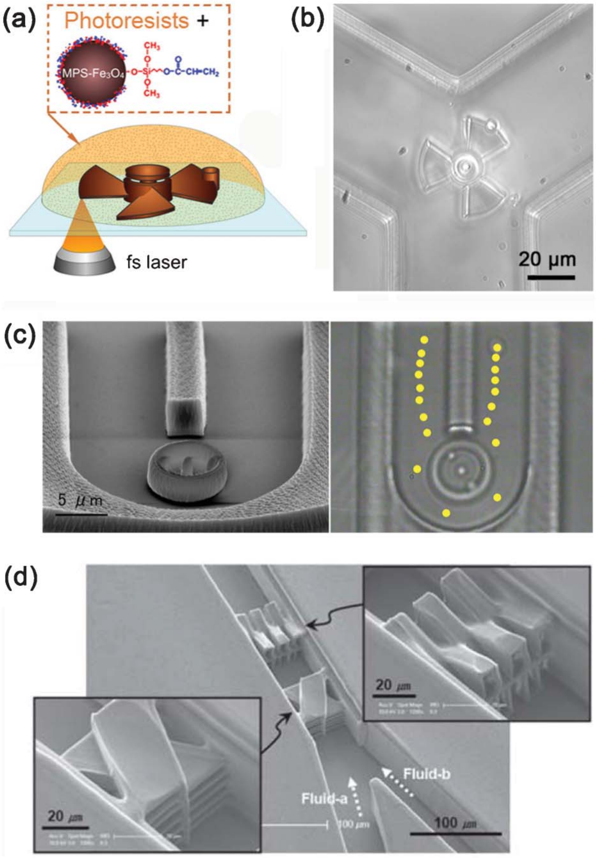

Fig. 7 (a) Schematic illustration of the TPP fabrication of magnetic photoresists for the preparation and remote control of a mixing device. (b) Optical microscopic image of the magnetic microturbine fabricated in a ''Y''-shaped microchannel. Reproduced from ref. 31 and 39 with the permission of RSC and Wiley. ©2010 by Wiley-VCH, ©2010 RSC. (c) SEM image of a disk microrotor and a U-shaped microchannel without an upper cover. Particle transportation by rotating the single-disk microrotor at 27 rpm. The white points show the positions of the microparticle taken at 2 s intervals. Reproduced from ref. 104 with the permission of AIP. ©2007 American Institute of Physics. (d) SEM images of a crossing manifold micromixer fabricated in a microchannel prepared by photolithography. Reproduced from ref. 38 with the permission of RSC. ©2011 by the Royal Society of Chemistry.

The integration of such an ''overpass'' structure at the junction of microfluidic channels could also be extended to three-channel junctions. In this case, the ''overpass'' should be designed into three layers. Theoretically speaking, this method is also suitable for some more complex situations, for instance five-channel junctions, however, considering the depth of such a junction, considerable difficulties would arise during the fabrication process.

Micromixers

The use of microfluidic chips is of benefit to the effective and convenient handling of chemical or biochemical reactions from reactant injection, and mixing to product collection. However, microfluidic mixing in a microchip channel is more difficult to control as compared with that in macroscopic reactors, because the laminar flow is dominant in the case of microfluidic channels. Therefore, an effective mixing device is necessary for microfluidic chips. With the help of TPP fabrication, both active[31,39,102,103] and passive[38] mixing devices can be readily prepared for microfluidic mixing.

As an active manner of mixing, magnetic stirring is widely used in macroscopic reactors. For microfluidic chips, magnetic mixing is also a good choice due to the non-contact and remotely controllable properties. For example, Xia *et al.*,[31] reported the TPP fabrication of a remotely controllable microturbine for microfluidic mixing. The fabrication was based on the successful preparation of a magnetic photoresist. As shown in Fig. 7a, to achieve a homogeneous dispersion of a magnetic source in a photopolymer, Fe_3O_4 nanoparticles were covalently coated with 3-(trimethoxysilyl)propyl methacrylate (MPS). Then the magnetic photoresist could be used for the TPP fabrication of various magnetic microstructures. Later, Tian *et al.*,[39] optimized the magnetic nanoparticles and a high performance mixing device for microfluidic chips was successfully fabricated. By using an extra rotating magnetic field, a rotating speed of 300 rpm was achieved. The development of this magnetic mixing device would undoubtedly contribute to the advance of multifunctional microfluidic devices. With the help of TPP processing, magnetic photoresists hold great promise for the fabrication of other high performance and magnetically controllable microdevices for LoC applications.

In addition to the magnetically driven route, optically driven microrotors have also been successfully developed as a remotely-controllable and mechanical contact-free device for microfluidics.[103–105] For example, Lin *et al.*, designed a turbine-like microrotor and made a quantitative analysis by computational fluid dynamics and semiclassical optics. The rotor could rotate at over 500 r min^{-1}, thus it could be used as a mixer in microfluidics.[103] Maruo and Inoue have recently developed a viscous micropump using a rotating disk. In the micropump, a disk microrotor, which has three columns as targets for the optical trap, is confined to a U-shaped microchannel, as shown in Fig. 7c.[104] The laser beam enabled rotation of the disk microrotor induces both a pressure gradient and steady flow along the curved channel, which is useful for continuous-flow chemical processes and the gentle sorting of biological samples.

For passive mixing devices, Lim *et al.*,[38] demonstrated a very typical example. In their work, a neo-conceptive 3D crossing manifold micromixer was fabricated in a microfluidic channel by sequential processes of photolithography and TPP fabrication. Shown in Fig. 7d is an SEM image of the crossing manifold micromixer. Two horizontally and vertically deposited crossing manifold micromixers have been fabricated in a "Y"-shaped microchannel. The wall thickness of the tube framework is designed to be ~1 μm for stability considerations. As a passive mixing device, the microfluids from two channels could be well mixed after passing through the crossing manifold. The location of the mixture in the channel could be chosen by changing the focus position of the laser according to the need of mixing action and the size was easy to adjust through the designed programs. In their work, ethanol with dye and water were used in a test of the mixing efficiency. A mixing ratio of 93.9% was obtained from the standard deviation, which is a little higher than that of the simulated result (90%). The *in situ* fabrication of mixing devices at desired positions of microfluidic chips will contribute to the development of advanced microfluidic devices with multifunctional integration.

Microheaters

In addition to the TPP integration of photopolymer microstructures inside microfluidic chips, metallic microdevices seem to be more important for chip functionalization. The use of metal structures in microfluidic chips is indispensable for achieving multifunctionality such as thermal and electronic conduction. However, it is known that metallic micropatterns are usually fabricated by conventional photolithography which is well witnessed by the development of integrated circuit (IC). For microfluidic chips, it is almost impossible to fabricate metallic microstructures inside a microfluidic channel by lithographic techniques. To achieve this end, femtosecond laser micronanofabrication provides an alternative approach. Typically, Xu *et al.*,[40] reported flexible nanowiring of silver on nonplanar substrates including microfluidic channels. The fundamental concept uses the FsLDW technique to fabricate silver micropatterns on desired substrates through two- or multiphoton absorption induced photoreduction of a silver precursor prepared from silver nitrate, ammonia, and trisodium citrate. As shown in Fig. 8a, the nonplanar nanowiring of silver inside a microfluidic channel directly leads to the formation of an electronic microheater that could be used to precisely control the local temperature of microfluids. Through careful control of laser power, the line width could be easily adjusted in the range of 125 to 500 nm. Moreover, the patterned silver nanowires maintained a low resistivity of about 1.6×10^{-7} Ω m^{-1}, which holds great promise for various circuitry and electronic interconnections.

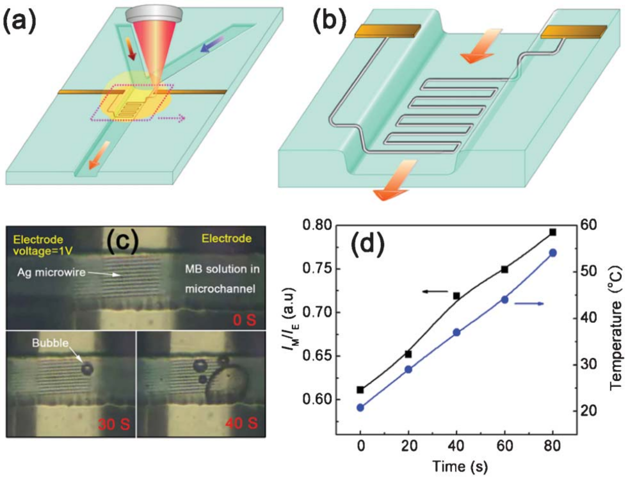

Fig. 8 (a, b) Schematic illustration of the fabrication of a silver microheater inside a microfluidic channel. (c) Heating test of a microheater fabricated inside a microchannel. Optical micrographs of the heating process. (d) Intensity ratio of monomer to excimer of PS-Na, used to quantitatively calculate the local temperature, and dependence of temperature on heating time. Reproduced from ref. 40 with the permission of Wiley-VCH. ©2010 Wiley-VCH.

As a microheater inside a microchannel, the silver heater shows ideal heating capability. Fig. 8c shows the heating capability of the silver microheater. For clearer observation, methylene blue trihydrate (MB; 0.1 mol L^{-1}) was injected into the microchannel. When a voltage of 1 V was supplied to this microheater, a bubble began to emerge in the surrounding solution within 30 s, indicating the rapid heating capability. With a constant voltage of 1.0 V, 54.8 °C can be reached from room temperature in 80 s following a linear relationship (Fig. 8d). The average heating rate is estimated to be 0.4 °C s^{-1}. The heating rate increases *versus* the voltage but a 5.0 V upper limit has been found for this circuit due to thermal stability of the silver microwire.

This microheater set directly inside a microchannel may find great potential in further miniaturized MEMS, microsensors, and LoC systems for highly localized temperature regulation. However, considering the stability for long time storage and the chemical activity in the presence of reagents, a protection layer is necessary for the practical use of such a silver microheater. Alternatively, other metal-based microheaters are also desired through the same technique for use in microfluidic devices.

SERS micromonitors

In recent years, surface enhanced Raman scattering (SERS) spectroscopy based on noble metal structures[103–108] has attracted much attention due to its capability of providing fingerprint information on various target molecules. However, to date, the SERS technique has not been widely used in microfluidic devices. A possible reason for this could be the lack of nanotechnology for the integration of SERS-active substrates inside microfluidic channels. Despite the existence of several reported works concerning on-chip SERS detection, it is still challenging to flexibly integrate SERS-active substrates inside microfluidic channels in a controlled fashion.

With the help of femtosecond laser fabrication, Xu *et al.*,[41] reported the flexible integration of a silver SERS monitor in a given microfluidic channel for high efficiency target molecule detection. Similar to the microheater discussed above, the mechanism for the fabrication of silver SERS substrates is also multiphoton absorption induced photoreduction of a silver salt solution. Fig. 9 shows the fundamental concept of the fabrication of a silver SERS substrate inside a microchannel and its application as a SERS monitor for target molecule detection. Taking advantage of the designability of laser processing, our SERS substrate could be created at any desired position and with arbitrary shapes. A magnified SEM image shows that the silver substrates were composed of vertical silver nanoplates with nanoparticles on each plate surface (Fig. 9c), and these hierarchical micronanostructures would contribute to an improved roughness and give rise to SERS enhancement. In tests of *p*-aminothiophenol as a probing molecule, a signal enhancement of 8 orders of magnitude was achieved with the silver substrate, indicating the excellent SERS enhancement. When two reactants pass the Y channel and mix together, these SERS substrates might be used for the detection of both the reactants and the products, making feasible the real-time monitoring of microfluidic reactions. This flexible integration of a silver SERS substrate would promote the use of the Raman spectral analysis in LoC systems.

Catalytic microreactors

With the rapid progress of LoC systems, the application of microfluidic devices has extended to a broad range of scientific fields. Especially, the unique features of microfluidics, such as low sample consumption, high activity, safety, environmental friendliness, and sensitivity, continuously stimulate research interest, bringing new investigations into this dynamic field, and heterogeneous catalysis is a typical example. For catalysis reactions, a microfluidic reactor not only allows the reactants to achieve full contact with the catalytic active sites in a confined space, and therefore contributes much higher catalytic activities as compared with macroscopic reactions, but it also provides an efficient and active experimental platform to make some chemical reactions possible with the help of catalysts. Therefore, catalytic microfluidic reactors are highly desired for the development of advanced LoC systems. However, technical difficulties in the fabrication and integration of catalyst embedded micro-reactors on tiny microfluidic devices constitute the main obstacle. Despite some previous works proving the possibility of fabricating on-chip catalytic reactors through dusting, sputtering or calcining various inorganic catalysts, the fabrication of catalytic microfluidic reactors also suffers from problems in both designability and stability. Recently, Xu *et al.*,[33] reported the on-chip fabrication of silver hierarchical structures as robust catalytically active sites for the reduction of 4-nitrophenol (4-NP) to 4-aminophenol (4-AP). In their work, the silver catalysts of the microfluidic reactor were fabricated by femtosecond laser photoreduction. Taking advantage of the designable nature of femtosecond laser fabrication, on-chip catalytic reactors show unique advantages of localized and homogeneous positioning of catalysts, high contact area between catalysts and reactants, as well as excellent stability against microfluidic impingement. In the catalytic reduction of 4-NP, the silver catalyst shows varying high activity. Even under a high flow rate of ~ 1 mL h^{-1}, the yield could reach almost 100%. More importantly, the silver catalytic active sites could also act as SERS active substrates for *in situ* monitoring of the chemical reaction. In this regard, the development of multifunctional catalytic microreactors might hold great potential for the investigation of catalysis mechanisms over a wide range of chemical reactions.

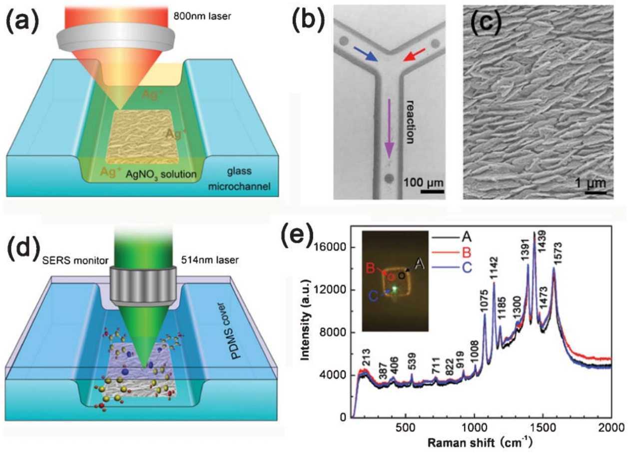

Fig. 9 (a) Schematic illustration of the fabrication of an on-chip SERS monitor. (b) Optical microscopic image of silver SERS substrates at different positions in a microchannel. (c) SEM image of the surface of a silver SERS substrate. (d) Schematic illustration of the use of this SERS monitor for target molecule detection. (e) Raman spectra of *p*-aminothiophenol (*p*-ATP) measured at different positions on the silver SERS substrate; the inset is an optical microscopic image. Reproduced from ref. 41 with the permission of RSC.

Later, Zarzar *et al.*,[42] reported the integration of catalytic nanostructured platinum and palladium within 3D fluidic architectures through multiphoton lithography. In their work, iron(III) oxalate was used as a photosensitive reducing agent for the generation of platinum and palladium microstructures. The as fabricated Pt and Pd micropatterns were composed of polycrystalline metallic nanoparticles that show excellent electronic, electrochemical, and catalytic properties. More importantly, they showed that site-specific decomposition of H_2O_2 catalyzed by the Pt microstructure could be used to drive microfluidic flow in three dimensions. As shown in Fig. 10, a Pt pattern was fabricated onto a glass substrate and then encased within a photocross-linked protein chamber containing a self-crossing spiral outlet. After the addition of H_2O_2, continuous and directed flow of oxygen could be observed due to Pt catalysis. Additionally, by directing the oxygen outflow into an asymmetric channel, negative pressure would be generated due to the periodically compressed and released oxygen bubble (Fig. 10b, c) which could be used to generate directed autonomous particle and fluid transport. Compared with silver structures, this MPA induced reduction of Pt and Pd microstructures process is more difficult to shape and the threshold energy is higher. The successful fabrication of Pt and Pd microstructures inside microfluidic devices has

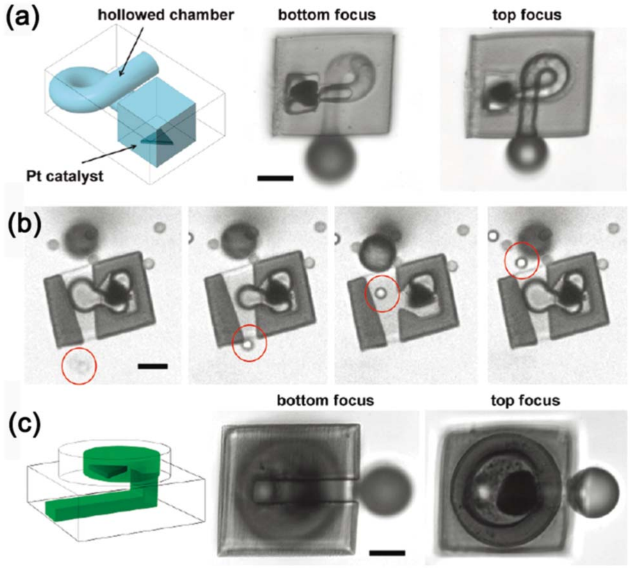

Fig. 10 (a) A Pt catalyst contained in a protein chamber directs gas through a self-crossing spiral channel. (b) The directional outflow of gas produced at a multiphoton lithography (MPL)-Pt catalyst contained in a microchamber pumps a 5 μm particle (circled in red) through the asymmetric channel over approximately 1 s. (c) An MPL-Pt catalyst printed inside the upper chamber of a 3D microchamber directs gas flow downward underneath the catalyst. Scale bars, 10 μm. Reproduced from ref. 42 with the permission of ACS. ©2012 by the American Chemical Society.

broadened the applications of metallic functional units in LoC devices. It not only provides a new approach to on-chip catalytic microreactors, but also endows conventional chips with more functionalities. With the integrated metallic structures, functionalities beyond catalysis, such as pumping, electrochemical or electronic properties, can be introduced into microfluidic systems in a controlled manner.

Conclusions and outlook

In the past two decades, micro total analysis systems (μTAS), represented by LoC devices, have seen thorough development due to their distinct advantages over macroscopic reactors. Microfluidic systems have already found broad applications in the fields of chemistry, physics, biology, materials science, pharmaceuticals, tissue engineering and iatrology. Additionally, with the rapid progress of interdisciplinary cooperation, more and more research interests will join this dynamic field. The gradually increased importance of this up-and-coming technique has led to higher requirements in chip complexity and compatibility. As a result, technical advances including both chip fabrication and multifunction integration have become more and more important.

As a powerful 3D processing tool, femtosecond laser micronanofabrication shows the advantages of designable and 3D processing capability, high spatial resolution, high accuracy, a wide array of processable materials, as well as high compatibility with other processing techniques. Therefore, the femtosecond laser fabrication technique has been considered as an advanced processing tool for prototyping various micronanostructures towards a wide range of applications. In this review, we have introduced this novel processing technique in the fabrication and functionalization of microfluidic devices. The fundamental principles of femtosecond laser micronanofabrication including micromachining and two-photon photopolymerization have been briefly introduced. By using the femtosecond laser fabrication technique, both the fabrication and functionalization of novel microfluidic chips are summarized. As typical examples, the integration of various functional units including microsieves, one-way microvalves, micro-overpasses, micromixers, microheaters, SERS monitors, and catalytic microreactors have been reviewed.

However, the capability of femtosecond laser micronanofabrication in chip functionalization is not limited to the above-mentioned examples. Considering the diversity of processable materials ranging from polymers, metals to oxide semiconductors, and the designable processing capability, there is room to design and integrate various functional units through this powerful micronanofabrication technique. At present, as compared with photolithographic techniques, the use of femtosecond laser fabrication in the field of chip preparation and functionalization is still at an early stage. With the rapidly increasing requirements for chip functionality and complexity, more and more functional units can be rationally designed and readily fabricated through this powerful micronanofabrication technique. Moreover, once novel photochemical schemes are developed, the processable materials would be extended to a much broader range, and thereafter, more functionalities could be realized in microfluidic chips far beyond chemical or biochemical analysis.

Additionally, with the rapid development of new-generation femtosecond lasers, the fabrication efficiencies and stabilities, as well as the cost will be significantly reduced, and thus concerns about the time consumption and expense would be overcome. It is believable that, using femtosecond laser micronanofabrication as a technical support, microfluidic chips may realize many additional functionalities, and therefore find broad applications in both scientific research and practical usage in the near future.

Acknowledgements

This work was supported by the National Science Foundation of China (Grant Nos. 90923037, 61008014 and 6078048). We also acknowledge the China Postdoctoral Science Foundation No. 20110490156 and the Hong Kong Scholar Program XJ2011014. The work was also supported by 2012 PhD interdisciplinary project No. 450060483105, Jilin University.

References

1 P. Yager, T. Edwards, E. Fu, K. Helton, K. Nelson, M. R. Tam and B. H. Weigl, *Nature*, 2006, **442**, 412.

2 G. M. Whitesides, *Nature*, 2006, **442**, 368.
3 D. Psaltis, S. R. Quake and C. Yang, *Nature*, 2006, **442**, 381.
4 D. Janasek, J. Franzke and A. Manz, *Nature*, 2006, **442**, 374.
5 J. El-Ali, P. K. Sorger and K. F. Jensen, *Nature*, 2006, **442**, 403.
6 A. J. de Mello, *Nature*, 2006, **442**, 394.
7 H. Craighead, *Nature*, 2006, **442**, 387.
8 J. Kong, L. Jiang, X. Su, J. Qin, Y. Du and B. Lin, *Lab Chip*, 2009, **9**, 1541.
9 H. Xie, B. Li, J. Qin, Z. Huang, Y. Zhu and B. Lin, *Electrophoresis*, 2009, **30**, 3514.
10 X. Gao, L. Jiang, X. Su, J. Qin and B. Lin, *Electrophoresis*, 2009, **30**, 2481.
11 Y. Zhang, H. Yu, J. Qin and B. Lin, *Biomicrofluidics*, 2009, **3**, 044105.
12 C. Li, X. Dong, J. Qin and B. Lin, *Anal. Chim. Acta*, 2009, **640**, 93.
13 Z. Li, K. Sun, M. Sunayama, Y. Matsuo, V. Mizeikis, R. Araki, K. Ueno, M. Abe and H. Misawa, *J. Chromatogr., A*, 2011, **1218**, 997.
14 K. Sun, N. Suzuki, Z. Li, R. Araki, K. Ueno, S. Juodkazis, M. Abe, S. Noji and H. Misawa, *Electrophoresis*, 2009, **30**, 4277.
15 R. G. Blazej, P. Kumaresan and R. A. Mathies, *Proc. Natl. Acad. Sci. U. S. A.*, 2006, **103**, 7240.
16 S. Huang, C. Li, B. Lin and J. Qin, *Lab Chip*, 2010, **10**, 2925.
17 J. Melin and S. R. Quake, *Annu. Rev. Biophys. Biomol. Struct.*, 2007, **36**, 213.
18 J. T. Nevill, R. Cooper, M. Dueck, D. N. Breslauer and L. P. Lee, *Lab Chip*, 2007, **7**, 1689.
19 A. Y. Lau, P. J. Hung, A. R. Wu and L. P. Lee, *Lab Chip*, 2006, **6**, 1510.
20 I. K. Dimov, L. Basabe-Desmonts, J. L. Garcia-Cordero, B. M. Ross, A. J. Ricco and L. P. Lee, *Lab Chip*, 2011, **11**, 845.
21 Z. Li, K. Sun, M. Sunayama, R. Araki, K. Ueno, M. Abe and H. Misawa, *Electrophoresis*, 2011, **32**, 3392.
22 W. Zheng, B. Jiang, D. Wang, W. Zhang, Z. Wang and X. Jiang, *Lab Chip*, 2012, **12**, 3441.
23 J. Wu and M. Gu, *J. Biomed. Opt.*, 2011, **16**, 080901.
24 S. Kawata, H.-B. Sun, T. Tanaka and K. Takada, *Nature*, 2001, **412**, 697.
25 A. Ovsianikov, A. Ostendorf and B. N. Chichkov, *Appl. Surf. Sci.*, 2007, **253**, 6599.
26 J. Wang, Y. He, H. Xia, L.-G. Niu, R. Zhang, Q.-D. Chen, Y.-L. Zhang, Y.-F. Li, S.-J. Zeng, J.-H. Qin, B.-C. Lin and H.-B. Sun, *Lab Chip*, 2010, **10**, 1993.
27 Z. B. Sun, X. Z. Dong, W. Q. Chen, S. Nakanishi, X. M. Duan and S. Kawata, *Adv. Mater.*, 2008, **20**, 914.
28 Y. Zhang, L. Guo, S. Wei, Y. He, H. Xia, Q. Chen, H.-B. Sun and F.-S. Xiao, *Nano Today*, 2010, **5**, 15.
29 Y. He, B.-L. Huang, D.-X. Lu, J. Zhao, B.-B. Xu, R. Zhang, X.-F. Lin, Q.-D. Chen, J. Wang, Y.-L. Zhang and H.-B. Sun, *Lab Chip*, 2012, **12**, 3866.
30 L. Wang, B.-B. Xu, Q.-D. Chen, Z.-C. Ma, R. Zhang, Q.-X. Liu and H.-B. Sun, *Opt. Lett.*, 2011, **36**, 3305.
31 H. Xia, J. Wang, Y. Tian, Q.-D. Chen, X.-B. Du, Y.-L. Zhang, Y. He and H.-B. Sun, *Adv. Mater.*, 2010, **22**, 3204.
32 L. Guo, H. Xia, H.-T. Fan, Y.-L. Zhang, Q.-D. Chen, T. Zhang and H.-B. Sun, *Opt. Lett.*, 2010, **35**, 1695.
33 B.-B. Xu, R. Zhang, X.-Q. Liu, H. Wang, Y.-L. Zhang, H.-B. Jiang, L. Wang, Z.-C. Ma, J.-F. Ku, F.-S. Xiao and H.-B. Sun, *Chem. Commun.*, 2012, **48**, 1680.
34 H. Xia, W.-Y. Zhang, F.-F. Wang, D. Wu, X.-W. Liu, L. Chen, Q.-D. Chen, Y.-G. Ma and H.-B. Sun, *Appl. Phys. Lett.*, 2009, **95**, 083118.
35 K. Sugioka and Y. Cheng, *Lab Chip*, 2012, **12**, 3576.
36 Y.-L. Zhang, Q.-D. Chen, H. Xia and H.-B. Sun, *Nano Today*, 2010, **5**, 435.
37 D. Wu, Q.-D. Chen, L.-G. Niu, J.-N. Wang, J. Wang, R. Wang, H. Xia and H.-B. Sun, *Lab Chip*, 2009, **9**, 2391.
38 T. W. Lim, Y. Son, Y. J. Jeong, D.-Y. Yang, H.-J. Kong, K.-S. Lee and D.-P. Kim, *Lab Chip*, 2011, **11**, 100.
39 Y. Tian, Y.-L. Zhang, J.-F. Ku, Y. He, B.-B. Xu, Q.-D. Chen, H. Xia and H.-B. Sun, *Lab Chip*, 2010, **10**, 2902.
40 B.-B. Xu, H. Xia, L.-G. Niu, Y.-L. Zhang, K. Sun, Q.-D. Chen, Y. Xu, Z.-Q. Lv, Z.-H. Li, H. Misawa and H.-B. Sun, *Small*, 2010, **6**, 1762.
41 B.-B. Xu, Z.-C. Ma, L. Wang, R. Zhang, L.-G. Niu, Z. Yang, Y.-L. Zhang, W.-H. Zheng, B. Zhao, Y. Xu, Q.-D. Chen, H. Xia and H.-B. Sun, *Lab Chip*, 2011, **11**, 3347.
42 L. D. Zarzar, B. S. Swartzentruber, J. C. Harper, D. R. Dunphy, C. J. Brinker, J. Aizenberg and B. Kaehr, *J. Am. Chem. Soc.*, 2012, **134**, 4007.
43 J. M. Fernández-Pradas, S. B. D. Serrano, J. L. Morenza and P. Serra, *Appl. Surf. Sci.*, 2011, 257.
44 G. C. B. Lee, J. Rasakanthan, P. D. Woolliams and K. Sugden, *Proc. SPIE*, 2012, **8427**, 84271K.
45 E. Mazur, L. Cerami, S. Nolte and C. B. Schaffer, *Femtosecond Laser Micromachining*, Trafford Publishing, Victoria, 2007.
46 G. Kumi, C. O. Yanez, K. D. Belfield and J. T. Fourkas, *Lab Chip*, 2010, **10**, 1057.
47 Q.-D. Chen, D. Wu, L.-G. Niu, J. Wang, X.-F. Lin, H. Xia and H.-B. Sun, *Appl. Phys. Lett.*, 2007, **91**, 171105.
48 B. C. Stuart, M. D. Feit, S. Herman, A. M. Rubenchik, B. W. Shore and M. D. Perry, *Phys. Rev. B: Condens. Matter*, 1996, **53**, 1749.
49 R. J. Dewhurst, *Meas. Sci. Technol.*, 2013, **24**, 012006.
50 Y. C. Lim, P. E. Boukany, D. F. Farson and L. J. Lee, *J. Micromech. Microeng.*, 2011, **21**, 015012.
51 K. L. N. Deepak, S. V. Rao and D. N. Rao, *Pramana*, 2010, **75**, 1221.
52 D. F. Farson, H. W. Choi, C. Lu and L. J. Lee, *J. Laser Appl.*, 2006, **18**, 210.
53 C. Wochnowski, Y. Cheng, Y. Hanada, K. Meteva, S. Metev, K. Sugioka, G. Sepold, F. Vollertsen and K. Midorikawa, *J. Laser Micro/Nanoeng.*, 2006, **1**, 195.
54 W. Pfleging, R. Adamietz, H. J. Bruckner, M. Bruns and A. Welle, *P. Soc. Photo-Opt. Ins.*, 2007, **6459**, 45907.
55 X. Zhu, A. Y. Naumov, D. M. Villeneuve and P. B. Corkum, *Appl. Phys. A: Mater. Sci. Process.*, 1999, **69**, S367.
56 D. J. Hwang, T. Y. Choi and C. P. Grigoropoulos, *Appl. Phys. A: Mater. Sci. Process.*, 2004, **79**, 605.
57 L. Shah, J. Tawney, M. Richardson and K. Richardson, *Appl. Surf. Sci.*, 2001, **183**, 151.
58 J.-T. Lee, M. C. George, J. S. Moore and P. V. Braun, *J. Am. Chem. Soc.*, 2009, **131**, 11294.
59 K. Sugioka, Y. Cheng and K. Midorikawa, *Appl. Phys. A: Mater. Sci. Process.*, 2005, **81**, 1.

60 H.-B. Sun and S. Kawata, in *NMR 3D Analysis Photopolymerization*, Springer, Berlin, Heidelberg, 2004, vol. 170, pp. 169.
61 S. Maruo and J. T. Fourkas, *Laser Photonics Rev.*, 2008, **2**, 100.
62 Y. Cao, Z. Gan, B. Jia, R. A. Evans and M. Gu, *Opt. Express*, 2011, **19**, 19486.
63 W.-K. Wang, Z.-B. Sun, M.-L. Zheng, X.-Z. Dong, Z.-S. Zhao and X.-M. Duan, *J. Phys. Chem. C*, 2011, **115**, 11275.
64 Y. Tian, Y.-L. Zhang, H. Xia, L. Guo, J.-F. Ku, Y. He, R. Zhang, B.-Z. Xu, Q.-D. Chen and H.-B. Sun, *Phys. Chem. Chem. Phys.*, 2011, **13**, 4835.
65 W. Xiong, Y. S. Zhou, X. N. He, Y. Gao, M. Mahjouri-Samani, L. Jiang, T. Baldacchini and Y. F. Lu, *Light: Sci. Appl.*, 2012, **1**, e6.
66 J. r. Koch, F. Korte, C. Fallnich, A. Ostendorf and B. N. Chichkov, *Opt. Eng.*, 2005, **44**, 051103.
67 H.-B. Sun, T. Tanaka, K. Takada and S. Kawata, *Appl. Phys. Lett.*, 2001, **79**, 1411.
68 J. Wang, H. Xia, B.-B. Xu, L.-G. Niu, D. Wu, Q.-D. Chen and H.-B. Sun, *Opt. Lett.*, 2009, **34**, 581.
69 T. Tanaka, H.-B. Sun and S. Kawata, *Appl. Phys. Lett.*, 2002, **80**, 312.
70 J. König, S. Nolte and A. Tünnermann, *Opt. Express*, 2005, **13**, 10597.
71 A. Marcinkevicius, S. Juodkazis, M. Watanabe, M. Miwa, S. Matsuo, H. Misawa and J. Nishii, *Opt. Lett.*, 2001, **26**, 277.
72 D. H. Kam, L. Shah and J. Mazumder, *J. Micromech. Microeng.*, 2011, **21**, 045027.
73 C. Florea and K. A. Winick, *J. Lightwave Technol.*, 2003, **21**, 246.
74 K. Miura, J. Qiu, H. Inouye, T. Mitsuyu and K. Hirao, *Appl. Phys. Lett.*, 1997, **71**, 3329.
75 L. Sudrie, M. Franco, B. Prade and A. Mysyrowicz, *Opt. Commun.*, 1999, **171**, 279.
76 L. Sudrie, M. Franco, B. Prade and A. Mysyrowicz, *Opt. Commun.*, 2001, **191**, 333.
77 E. N. Glezer, M. Milosavljevic, L. Huang, R. J. Finlay, T. H. Her, J. P. Callan and E. Mazur, *Opt. Lett.*, 1996, **21**, 2023.
78 C. B. Schaffer, A. O. Jamison and E. Mazur, *Appl. Phys. Lett.*, 2004, **84**, 1441.
79 E. N. Glezer and E. Mazur, *Appl. Phys. Lett.*, 1997, **71**, 882.
80 K. Sugioka, Y. Cheng and K. Midorikawa, *J. Phys. Conf. Ser.*, 2007, **59**, 533.
81 J. A. Dharmadhikari, A. K. Dharmadhikari, A. Bhatnagar, A. Mallik, P. C. Singh, R. K. Dhaman, K. Chalapathi and D. Mathur, *Opt. Commun.*, 2011, **284**, 630.
82 M. Kim, D. J. Hwang, H. Jeon, K. Hiromatsu and C. P. Grigoropoulos, *Lab Chip*, 2009, **9**, 311.
83 V. Maselli, J. R. Grenier, S. Ho and P. R. Herman, *Opt. Express*, 2009, **17**, 11719.
84 C.-H. Lin, L. Jiang, H. Xiao, Y.-H. Chai, S.-J. Chen and H.-L. Tsai, *Opt. Lett.*, 2009, **34**, 2408.
85 L. L. Qiao, F. He, C. Wang, Y. Cheng, K. Sugioka and K. Midorikawa, *Appl. Phys. A: Mater. Sci. Process.*, 2011, **102**, 179.
86 Y. Li and S.-l. Qu, *Mater. Lett.*, 2010, **64**, 1427.
87 M. Masuda, K. Sugioka, Y. Cheng, N. Aoki, M. Kawachi, K. Shihoyama, K. Toyoda, H. Helvajian and K. Midorikawa, *Appl. Phys. A: Mater. Sci. Process.*, 2003, **76**, 857.
88 K. Sugioka, M. Masuda, T. Hongo, Y. Cheng, K. Shihoyama and K. Midorikawa, *Appl. Phys. A: Mater. Sci. Process.*, 2004, **79**, 815.
89 Y. Cheng, K. Sugioka and K. Midorikawa, *Opt. Express*, 2005, **13**, 7225.
90 M. Masuda, K. Sugioka, Y. Cheng, N. Aoki, M. Kawachi, K. Shihoyama, K. Toyoda, H. Helvajian and K. Midorikawa, *Appl. Phys. A: Mater. Sci. Process.*, 2003, **76**, 857.
91 K. Sugioka, Y. Cheng and K. Midorikawa, *Appl. Phys. A: Mater. Sci. Process.*, 2005, **81**, 1.
92 Y. Kondo, J. Qiu, T. Mitsuyu, K. Hirao and T. Yoko, *Jpn. J. Appl. Phys.*, 1999, **38**, L1146.
93 Y. Ju, Y. Liao, L. Zhang, Y. Sheng, Q. Zhang, D. Chen, Y. Cheng, Z. Xu, K. Sugioka and K. Midorikawa, *Microfluid. Nanofluid.*, 2011, **11**, 111.
94 Y. Liao, J. Song, E. Li, Y. Luo, Y. Shen, D. Chen, Y. Cheng, Z. Xu, K. Sugioka and K. Midorikawa, *Lab Chip*, 2012, **12**, 746.
95 H. W. Choi, S. Bong, D. F. Farson, C. M. Lu and L. J. Lee, *J. Laser Appl.*, 2009, **21**, 196.
96 R. M. Vazquez, R. Osellame, D. Nolli, C. Dongre, H. van den Vlekkert, R. Ramponi, M. Pollnau and G. Cerullo, *Lab Chip*, 2009, **9**, 91.
97 R. M. Vazquez, R. Osellame, M. Cretich, M. Chiari, C. Dongre, H. J. W. M. Hoekstra, M. Pollnau, H. v. d. Vlekkert, R. Ramponi and G. Cerullo, *Anal. Bioanal. Chem.*, 2009, **393**, 1209.
98 H. Zhang, S. Ho, S. M. Eaton, J. Li and P. R. Herman, *Opt. Express*, 2008, **16**, 14015.
99 W. Pfleging, M. Torge, M. Bruns, V. Trouillet, A. Welle and S. Wilson, *Appl. Surf. Sci.*, 2009, **255**, 5453.
100 J. K. Gansel, M. Thiel, M. S. Rill, M. Decker, K. Bade, V. Saile, G. von Freymann, S. Linden and M. Wegener, *Science*, 2009, **325**, 1513.
101 W. Zhou, S. M. Kuebler, K. L. Braun, T. Yu, J. K. Cammack, C. K. Ober, J. W. Perry and S. R. Marder, *Science*, 2002, **296**, 1106.
102 R. Di Leonardo, A. Búzás, L. Kelemen, G. Vizsnyiczai, L. Oroszi and P. Ormos, *Phys. Rev. Lett.*, 2012, **109**, DOI: 10.1103/PhysRevLett.109.034104.
103 X.-F. Lin, G.-Q. Hu, Q.-D. Chen, L.-G. Niu, Q.-S. Li, A. Ostendorf and H.-B. Sun, *Appl. Phys. Lett.*, 2012, **101**, 113901.
104 S. Maruo and H. Inoue, *Appl. Phys. Lett.*, 2007, **91**, 084101.
105 S. Maruo and H. Inoue, *Appl. Phys. Lett.*, 2006, **89**, 144101.
106 Y.-H. Su, Y.-F. Ke, S.-L. Cai and Q.-Y. Yao, *Light: Sci. Appl.*, 2012, **1**, e14.
107 H. Cho, B. Lee, G. L. Liu, A. Agarwal and L. P. Lee, *Lab Chip*, 2009, **9**, 3360.
108 B.-B. Xu, Z.-C. Ma, H. Wang, X.-Q. Liu, Y.-L. Zhang, X.-L. Zhang, R. Zhang, H.-B. Jiang and H.-B. Sun, *Electrophoresis*, 2011, **32**, 3378.